AGU PUBLICATIONS

Radio Science

RESEARCH ARTICLE
10.1002/2016RS006027

Key Points:
- Accurate analysis and design of E-plane multiport waveguide junctions
- Compensation of the use of low-cost manufacture techniques
- Design of a great variety of waveguide components used in modern telecommunication systems

Correspondence to:
A. A. San-Blas,
aasanblas@umh.es

Citation:
San-Blas, A. A., J. M. Roca, S. Cogollos, J. V. Morro, V. E. Boria, and B. Gimeno (2016), Compensation of the impact of low-cost manufacturing techniques in the design of E-plane multiport waveguide junctions, *Radio Sci.*, *51*, 619–628, doi:10.1002/2016RS006027.

Received 23 MAR 2016
Accepted 13 MAY 2016
Accepted article online 18 MAY 2016
Published online 7 JUN 2016

Compensation of the impact of low-cost manufacturing techniques in the design of E-plane multiport waveguide junctions

A. A. San-Blas[1], J. M. Roca[1], S. Cogollos[2], J. V. Morro[2], V. E. Boria[2], and B. Gimeno[3]

[1]Departamento de Ingeniería de Comunicaciones, Universidad Miguel Hernández de Elche, Elche, Spain, [2]Departamento de Comunicaciones-iTEAM, Universitat Politècnica de València, Valencia, Spain, [3]Departamento de Física Aplicada y Electromagnetismo-ICMUV, Universidad de Valencia, Valencia, Spain

Abstract In this work, a full-wave tool for the accurate analysis and design of compensated E-plane multiport junctions is proposed. The implemented tool is capable of evaluating the undesired effects related to the use of low-cost manufacturing techniques, which are mostly due to the introduction of rounded corners in the cross section of the rectangular waveguides of the device. The obtained results show that, although stringent mechanical effects are imposed, it is possible to compensate for the impact of the cited low-cost manufacturing techniques by redesigning the matching elements considered in the original device. Several new designs concerning a great variety of E-plane components (such as right-angled bends, T-junctions and magic-Ts) are presented, and useful design guidelines are provided. The implemented tool, which is mainly based on the boundary integral-resonant mode expansion technique, has been successfully validated by comparing the obtained results to simulated data provided by a commercial software based on the finite element method.

1. Introduction

Modern microwave equipment present in many telecommunication systems, such as satellite communication payloads and long-range radar applications, usually demands for low-cost technologies and wider operating bandwidths in order to meet the stringent requirements of current high-frequency communication systems [*Uher et al.*, 1993; *Boria and Gimeno*, 2007; *Park et al.*, 2009]. Among them, multiport waveguide junctions are key building blocks of many passive components. They play an increasingly important role in the design of a great variety of microwave and millimeter-wave devices, such as power dividers/combiners [*Chu et al.*, 2014; *Xu et al.*, 2015; *Cano et al.*, 2016], directional couplers [*Leal-Sevillano et al.*, 2013], E-plane T-junctions [*Berdnik et al.*, 2015; *Helszajn*, 2016], double-ridge waveguide power dividers [*Ruiz et al.*, 2015], waveguide bends, and magic-T junctions [*San-Blas et al.*, 2007; *Kamandi et al.*, 2015]. Low-cost manufacturing techniques, such as milling, do usually have a negative impact on the overall electrical performance of the fabricated device, due to the introduction of rounded corners in the cross section of the waveguide ports of the considered component [*Cogollos et al.*, 2003a]. The consequences of such degradation may include a shift in the frequency response of the device, an important reduction of the usable bandwidth, and a decrement of the predicted return losses [*San-Blas et al.*, 2015].

An accurate investigation of the aforementioned undesired effects on compensated H-plane multiport waveguide junctions was performed by the authors in *San-Blas et al.* [2015]. In such contribution, a full-wave computer-aided design (CAD) tool was developed for analyzing the degradation of the electrical performance of different H-plane components (e.g., compensated right-angled bends, T-junctions, and turnstile junctions) due to the mechanization effects associated with low-cost production techniques. The authors concluded that although the wideband performance of such devices could be critically reduced as a result of the cited mechanization effects, it was possible to compensate for this degradation by properly redesigning the component (i.e., by changing the dimensions and/or the relative position of the post used to match the device). Furthermore, the scope of such work was limited to H-plane devices, where all involved planar junctions were restricted to discontinuities between standard rectangular waveguides and arbitrary waveguides (i.e., rectangular waveguides with rounded corners). Nevertheless, if E-plane rectangular waveguide components are

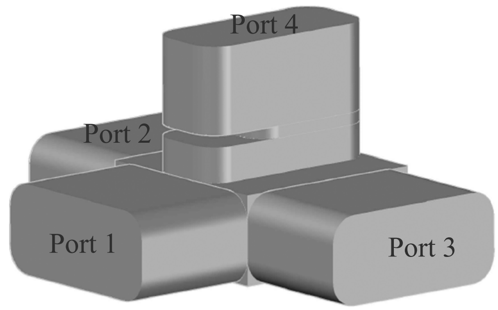

Figure 1. Magic-T junction with a matching iris in the E-plane arm. Rounded corners have been considered in all the rectangular waveguides connected to the ports of the device.

going to be considered, the optimization of the frequency response of the designed junction usually requires the introduction of a matching iris in the E-plane arm of the structure [*San-Blas et al.*, 2007]. As a consequence, if such E-plane component is manufactured by means of low-cost production techniques, the planar junctions between the arbitrary waveguides (i.e., rectangular waveguides with rounded corners) present in the aforementioned E-plane arm of the structure need to be rigorously analyzed. For instance, a magic-T junction with rounded corners in all the rectangular waveguide access ports has been depicted in Figure 1. Note that several discontinuities between arbitrarily shaped waveguides can be observed in the E-plane arm of the junction.

The main aim of this work is to present a novel full-wave CAD tool able to cope with the accurate analysis and design of compensated E-plane multiport junctions (right-angled bends, T-junctions, and magic-Ts) considering the introduction of rounded corners in the cross section of all the rectangular waveguides connected to the ports of the analyzed junction. It is worthwhile to mention that this work involves a significant theoretical extension compared with an authors' previous contribution presented in *San-Blas et al.* [2015] since, in this new case, planar junctions between arbitrarily shaped waveguides must be considered to achieve a rigorous full-wave analysis of the components. Furthermore, note that with the aim of optimizing their electrical response, the designed E-plane multiport junctions, such as the magic-T depicted in Figure 1, will be compensated by inserting a cylindrical metallic post that can be placed at an arbitrary position within the component [see *San-Blas et al.*, 2007, 2015].

The full-wave analysis of the new designed devices is based on the combination of the 2-D and 3-D BI-RME (Boundary Integral-Resonant Mode Expansion) methods. In particular, the 2-D BI-RME technique [*Conciauro et al.*, 1984; *Cogollos et al.*, 2003b] will be employed to obtain the modal charts of the arbitrary waveguides of the component (i.e., rectangular waveguides with rounded corners), while the 3-D BI-RME method [*Arcioni et al.*, 2002; *Mira et al.*, 2005] will provide us with a wideband multimode characterization of the core of the device (i.e., a boxed cavity loaded with a cylindrical metallic post) in terms of an equivalent generalized admittance matrix. In addition, an efficient integral equation technique for the full-wave characterization of the planar junctions between the arbitrarily shaped waveguides will be also used [*Gerini et al.*, 1998].

In order to validate the proposed method, several compensated E-plane multiport junctions are analyzed and designed, considering the introduction of rounded corners in the rectangular waveguide access ports of the components. The obtained results provide useful design guidelines to optimize the electrical performance of the investigated junctions, even though stringent mechanical effects (i.e., high values of the rounded corners' radius) are imposed. As a consequence, the broadband operation of a great variety of low-cost manufactured E-plane components can be restored by properly redesigning the junction, so that a microwave designer can accurately evaluate the final electrical response of the device prior to its manufacturing. The obtained results are successfully compared with numerical data extracted from a commercial software based on the finite element method, thus demonstrating the accuracy of the implemented software tool.

2. Full-Wave Analysis of Compensated E-Plane Multiport Junctions Considering the Effect of Low-Cost Manufacturing Techniques

The full-wave analysis of compensated E-plane multiport components can be readily performed by means of the so-called segmentation technique, which consists of decomposing the analysis of a complete waveguide structure into the characterization of its elementary key building blocks. To illustrate this concept in more detail, let us consider the compensated E-plane T-junction depicted in Figure 2, where a partial-height cylindrical metallic post (radius r, height h, and off-centered position, x_0, z_0) and a matching iris (width a_{iris}, thickness t_{iris}, and height h_{iris}) have been inserted in the structure with the aim of achieving an optimum broadband operation [*San-Blas et al.*, 2007]. Rounded corners of radius R have also been considered in the

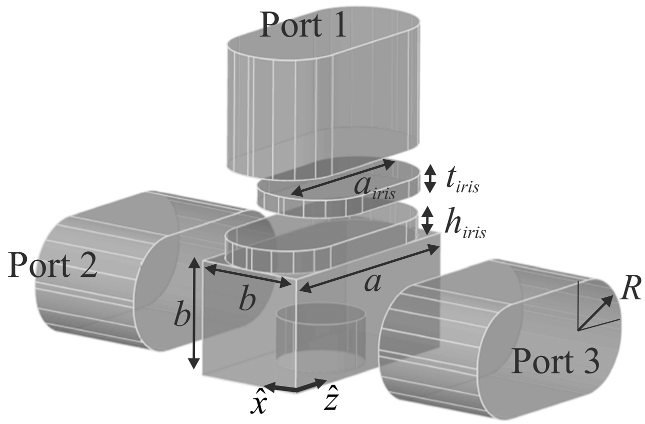

Figure 2. Compensated E-plane T-junction with rounded corners in the rectangular waveguides of the device.

cross section of the rectangular waveguide access ports of the cited junction, in order to take into account the use of low-cost fabrication techniques. Moreover, note that the different building blocks of the E-plane T-junction shown in Figure 2 have been disassembled for the sake of clarity.

The multimode analysis of the component starts from the electromagnetic characterization of a boxed cavity (whose dimensions are $a \times b \times b$ in Figure 2) loaded with a partial-height cylindrical metallic post placed at an arbitrary position (x_0, z_0) on the base surface of such cavity. To this aim, the 3-D BI-RME method [*Mira et al.*, 2005] has been implemented by considering N standard rectangular waveguide access ports of dimensions $a\times b$ (for instance, $N=4$ in the magic-T junction shown in Figure 1, and $N = 3$ in the structure shown in Figure 2). The 3-D BI-RME method is a very efficient algorithm for the full-wave analysis of arbitrarily shaped components that relates the pole expansion of the admittance parameters of the device to the resonant modes of the cavity obtained after short circuiting the access ports of the structure. Therefore, the method finally provides a rigorous electromagnetic characterization of the investigated component in terms of an equivalent generalized admittance matrix, expressed as a pole expansion in the s domain as follows:

$$\mathbf{Y} = \frac{1}{s\eta}\mathbf{A} + \frac{s}{\eta}\mathbf{B} - \frac{s^3}{\eta}\sum_{i=1}^{Q}\frac{\mathbf{v}^{(i)}\mathbf{v}_{\mathrm{T}}^{(i)}}{s^2 + k_i^2} \tag{1}$$

where $s=jw\sqrt{\mu\epsilon}$; matrices **A** and **B** are real, symmetric and frequency independent; η is the wave impedance; $k_i (i = 1, \dots, Q)$ represent the first Q resonant wave numbers of the short-circuited cavity, and vectors $\mathbf{v}^{(i)}$ are related to the eigenvectors associated to k_i (see *Arcioni et al.* [2002] for more details on this formulation).

Once the central boxed cavity has been characterized, the next step consists of analyzing the planar waveguide junctions found in the component. It is important to mention the different types of planar waveguide junctions present in the T-junction shown in Figure 2. On the one hand, several planar junctions between a rectangular waveguide (i.e., a face of the central boxed cavity) and an arbitrarily shaped waveguide (i.e., rectangular waveguide with rounded corners) can be observed in both the collinear and the E-plane arms of the T-junction. The full-wave analysis of such planar junctions was rigorously performed in *San-Blas et al.* [2015], by combining the integral equation technique described in *Gerini et al.* [1998], and the 2-D BI-RME method [*Cogollos et al.*, 2003b], which is used to derive the modal chart of the arbitrary waveguides. On the other hand, and in contrast to the work developed by the authors in *San-Blas et al.* [2015], new planar junctions between two arbitrary waveguides can be observed in the E-plane arm of the device depicted in Figure 2, due to the presence of the matching iris. The analysis of this type of junctions can also be carried out by implementing the integral equation technique above mentioned, which provides a full-wave characterization of the discontinuity in terms of an equivalent generalized impedance matrix (GIM).

In order to derive such GIM, the coupling coefficients between the modal sets of the waveguides involved in the considered junction need to be first calculated. Note that, as this computation always involved a standard rectangular waveguide in the work performed in *San-Blas et al.* [2015], the procedure detailed in *Arcioni* [1996] could be implemented with the aim of achieving an efficient software tool. However, since the design of E-plane components force the appearance of planar junctions between arbitrarily shaped waveguides, the technique described in *Arcioni* [1996] cannot be directly used and a new strategy is required to efficiently compute the aforementioned modal coupling coefficients. Such strategy starts from expressing the vector modal functions $\mathbf{e}^{(A)}$ of the arbitrarily shaped waveguides in terms of the vector modal functions $\mathbf{e}^{(R)}$ of their corresponding external rectangular contours:

$$\mathbf{e}_p^{(A)} = \sum_{q=1}^{\infty} \gamma_{p,q}^{(A,R)}\ \mathbf{e}_q^{(R)}, \tag{2}$$

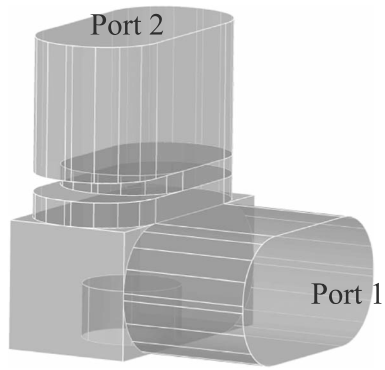

Figure 3. Compensated E-plane right-angled bend with rounded corners in the rectangular waveguides of the component.

where the auxiliary coupling coefficients $\gamma_{p,q}^{(A,R)}$ can be readily computed by using the method explained in *Arcioni* [1996]:

$$\gamma_{p,q}^{(A,R)} = \int_{S_A} \mathbf{e}_p^{(A)} \cdot \mathbf{e}_q^{(R)} \, dS. \tag{3}$$

The desired modal coupling coefficient $\Gamma_{m,n}$ between the mth vector modal function of the arbitrarily shaped waveguide A_1 (bigger waveguide whose external rectangular contour is denoted by R_1) and the nth vector modal function of the arbitrarily shaped waveguide A_2 (smaller waveguide whose external rectangular contour is denoted by R_2) can be now derived in the following form:

$$\begin{aligned}\Gamma_{m,n} &= \int_{S_{A_2}} \mathbf{e}_m^{(A_1)} \cdot \mathbf{e}_n^{(A_2)} \, dS = \int_{S_{R_2}} \left(\sum_{i=1}^{\infty} \gamma_{m,i}^{(A_1,R_1)} \, \mathbf{e}_i^{(R_1)} \right) \cdot \left(\sum_{j=1}^{\infty} \gamma_{n,j}^{(A_2,R_2)} \, \mathbf{e}_j^{(R_2)} \right) dS \\ &= \sum_{i=1}^{\infty} \sum_{j=1}^{\infty} \gamma_{m,i}^{(A_1,R_1)} \gamma_{n,j}^{(A_2,R_2)} \int_{S_{R_2}} \mathbf{e}_i^{(R_1)} \cdot \mathbf{e}_j^{(R_2)} \, dS.\end{aligned} \tag{4}$$

Note that the last surface integral in (4) involves vector modal functions related to standard rectangular waveguides and, therefore, it can be analytically computed. Moreover, the authors have verified that only 150–200 terms are typically needed to achieve accurate and convergent results in the previous twofold summation, provided that 20–30 accessible modes are considered in the equivalent multimode network.

Once the expressions for the wideband matrices of all the elementary blocks of the structure have been derived using the proposed techniques, a proper connection of the obtained generalized admittance and impedance matrices must be performed in order to compute the electrical response of the whole component. As a result, an equivalent hybrid immittance matrix can be obtained for the characterization of the entire device, thus requiring the inversion of just one matrix per frequency point, and consequently minimizing the overall CPU requirements.

3. Results and Discussion

The objective of this section is to validate the implemented tool for the full-wave analysis and design of compensated E-plane multiport junctions (e.g., right-angled bends, T-junctions, and magic-Ts) considering the

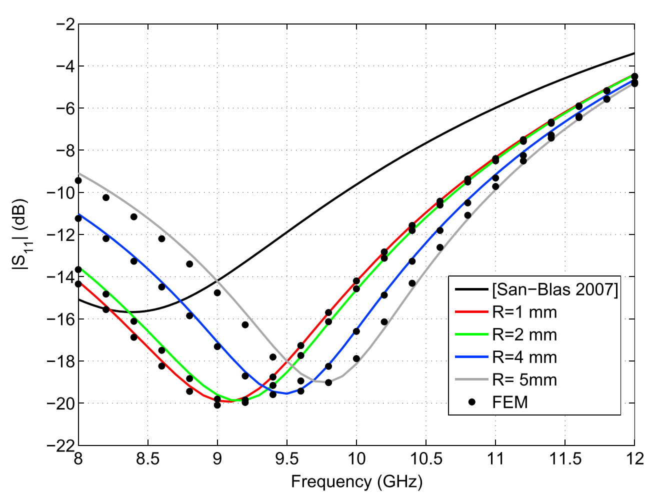

Figure 4. Return losses of a compensated E-plane right-angled bend as a function of the radius *R* of the rounded corners.

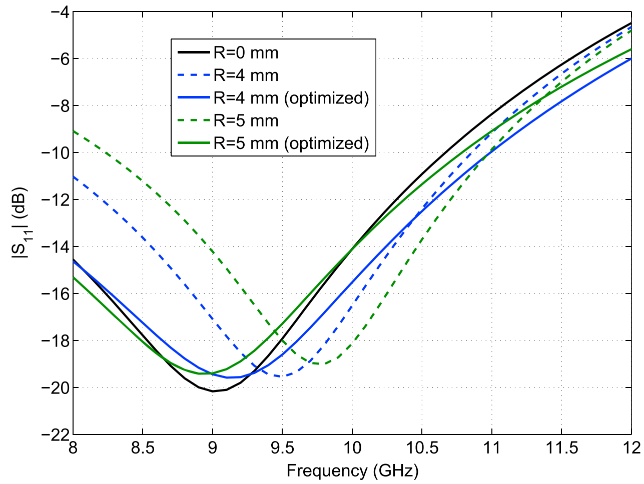

Figure 5. Return losses of the redesigned E-plane right-angled bend.

mechanization effects associated to low-cost manufacturing techniques (i.e., the introduction of rounded corners). The new designs presented in this work have required the use of 20 accessible modes in the equivalent multimode network, 290 resonant modes in the central boxed cavity, and a maximum of 600 modes in the external rectangular waveguide box used to characterize the arbitrarily shaped waveguides. Regarding the integral equation technique used for the analysis of the planar waveguide junctions, we have required a maximum of 100 basis functions and 260 terms for summing the infinite series inherent to the cited technique. Furthermore, the design guidelines described in *Hirokawa et al.* [1991] have been followed in order to optimize the electrical response of the designed components. The accuracy of the proposed method has been successfully validated by comparing the obtained results with simulated data extracted from a commercial software based on the finite element method (FEM).

3.1. Design of Compensated E-Plane Right-Angled Bends

First, we proceed to validate the proposed tool by analyzing a compensated E-plane right-angled bend implemented in WR-90 rectangular waveguide (a = 22.86 mm, b = 10.16 mm), as the one represented in Figure 3.

A cylindrical metallic post of radius r = 3.75 mm, height h = 3.08 mm, and relative position (x_0, z_0) = (6.31, 11.48) mm (according to the axis system depicted in Figure 2) has been used to compensate the junction. In addition, a matching iris has been inserted into the component to optimize its broadband operation. The dimensions of the iris, referred to the notation indicated in Figure 2, are a_{iris} = 20.32 mm, t_{iris} = 2.15 mm, and h_{iris} = 8.1 mm. Moreover, the rectangular waveguides present in the component have been perturbed by introducing rounded corners of radius R.

The electrical performance of the designed E-plane bend, as a function of the radius R of the rounded corners, is presented in Figure 4, where the obtained simulated data are successfully compared to the results provided by a finite element method software. The results related to the case $R = 0$ (absence of rounded corners), which have not been included in such figure for the sake of clarity, are very close to the data obtained for the case $R = 1$ mm. Furthermore, the return losses related to an authors' previous design concerning a compensated E-plane bend without rounded corners ($R = 0$) are also included in Figure 4 for comparison purposes (see the solid black curve) [*San-Blas et al.*, 2007]. It is important to note, by comparing the cited black curve and the curve related to the case $R = 1$ mm (whose results are very close to the case $R = 0$), that an improved initial design (for the cited case of $R = 0$) has been achieved in this new work.

Table 1. New Dimensions of the Matching Elements (Post and Iris) Used in the Redesign of the E-Plane Right-Angled Bend

Radius R	r (mm)	h (mm)	x_0 (mm)	z_0 (mm)	a_{iris} (mm)	t_{iris} (mm)	h_{iris} (mm)
R = 4 mm	3.75	3.05	6.4	11.43	21.15	2.79	7.8
R = 5 mm	3.75	2.56	6.4	11.43	21.45	2.79	7.8

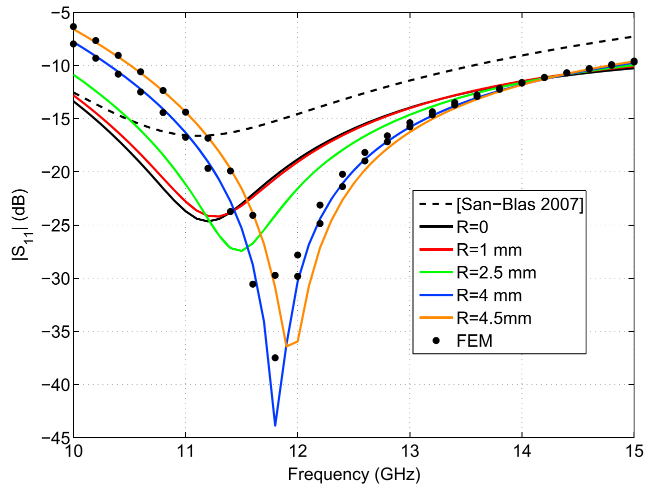

Figure 6. Return losses of a compensated E-plane T-junction as a function of the radius *R* of the rounded corners.

In view of the obtained results, it is possible to conclude that the overall electrical performance of the device deteriorates as the radius of the rounded corners increases. The negative effect is noteworthy in the cases $R = 4$ mm and $R = 5$ mm. Nevertheless, even in these cases with stringent mechanical constraints, the broadband operation of the low-cost manufactured E-plane bend can be almost restored by properly redesigning the junction. In this particular case, we propose to redesign the dimensions and the relative position of the cylindrical post, and also the different dimensions related to the auxiliary iris. The return losses related to these new designs are shown in Figure 5, where it is possible to observe that the overall electrical performance of the device has been almost restored (compared to the case $R = 0$ that has been now included in the figure), when high values of the rounded corners ($R = 4$ mm and $R = 5$ mm) are considered. The dimensions of the cylindrical post (its radius r, height h, and relative position x_0, z_0) and the dimensions that define the matching iris (its width a_{iris}, thickness t_{iris}, and height h_{iris}), related to such new designs, are collected in Table 1.

It is important to note that the electrical performance of the device is sensitive to the ratio R/b. In particular, when $R > b/4$, further optimizations may be needed in order to restore the broadband operation of the component. Finally, it should be observed that the CPU time required for the computation of a complete frequency response (150 points) was only 28.7 s (Intel Core i3@3.1 GHz with 4 GB RAM), thus demonstrating the computational efficiency of the developed CAD tool (Ansys HFSS, the commercial tool based on FEM used for validation purposes, took about 1 min per frequency point).

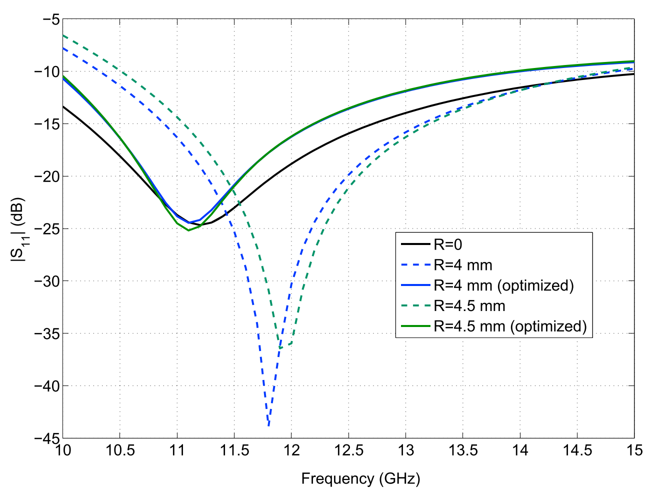

Figure 7. Return losses of the redesigned compensated E-plane T-junction.

Table 2. New Dimensions of the Matching Elements (Post and Iris) Employed in the Redesign of the E-Plane T-Junction

Radius R	r (mm)	h (mm)	a_{iris} (mm)	t_{iris} (mm)	h_{iris} (mm)
$R = 4$ mm	3.78	4.08	15.17	1.25	2.74
$R = 4.5$ mm	3.78	4.03	15.21	0.9	2.98

3.2. Design of Compensated E-Plane T-Junctions

E-plane T-junctions are extensively used as power dividers in modern diplexers and multiplexers [*Zhang et al.*, 2010; *Chen et al.*, 2014]. In this section, we present a new design of a compensated E-plane T-junction, considering rounded corners of radius R in the rectangular waveguides of the component (see Figure 2). The T-junction has been implemented in WR-75 rectangular waveguide ($a = 19.05$ mm, $b = 9.525$ mm), using a cylindrical post of dimensions (in mm): $r = 3.6$, $h = 3.96$. In this case, the best performance has been found when the post is located in a centered position $(x_0, z_0) = (b/2, a/2)$. On the other hand, the dimensions of the matching iris are (in mm): $a_{iris} = 15.12$, $t_{iris} = 1.45$, and $h_{iris} = 1.85$. The electrical response of the T-junction, as a function of the radius R of the rounded corners, is shown in Figure 6, where an excellent agreement with the data provided by the finite element method software is again observed.

First of all, it should be noted that this new design has improved the electrical performance of the component (case for $R = 0$) compared to an authors' previous design presented in *San-Blas et al.* [2007] (see the dashed black curve in Figure 6). Moreover, in contrast to the outcome of the study about H-plane T-junctions performed by the authors in *San-Blas et al.* [2015], where the introduction of the rounded corners did not significantly affect the electrical response of the device, the degradation of the overall frequency response is

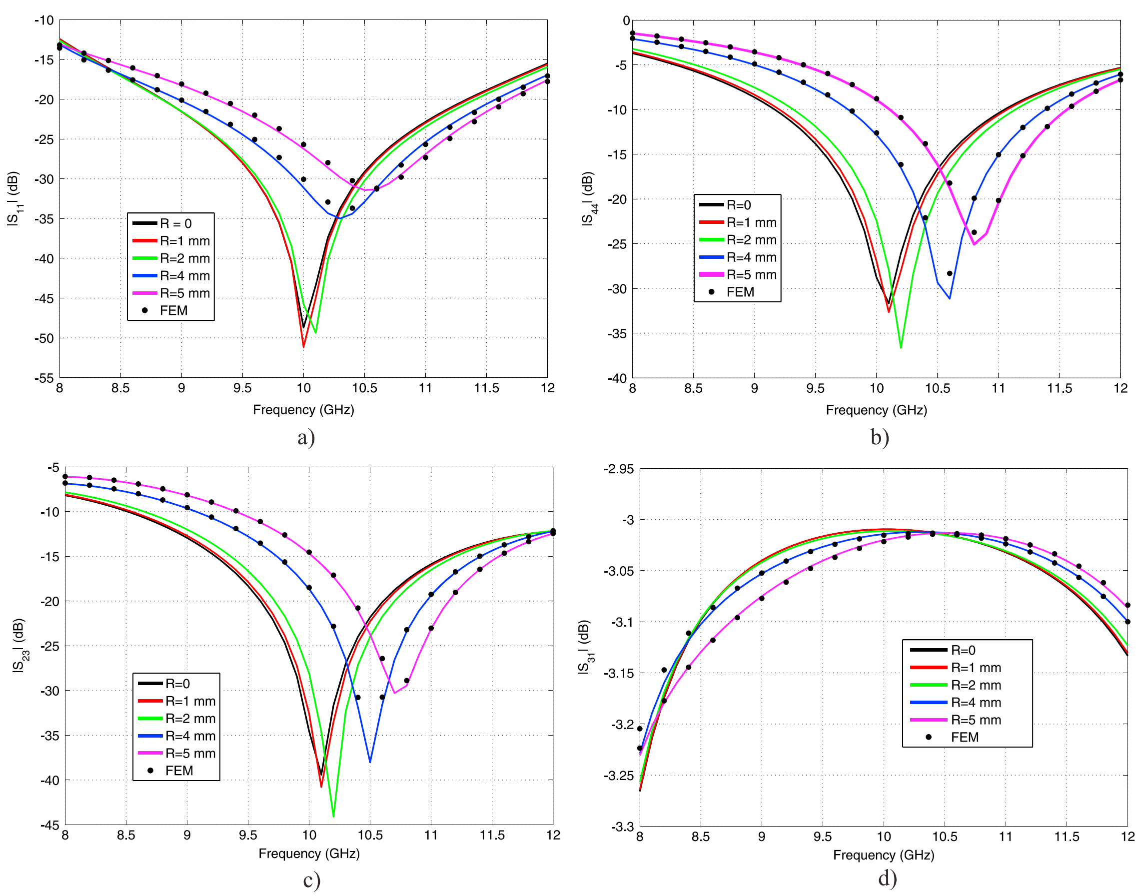

Figure 8. S-parameters of a compensated magic-T junction considering rounded corners of radius R in the rectangular waveguides of the device. (a) Magnitude (dB) of S_{11}. (b) Magnitude (dB) of S_{44}. (c) Magnitude (dB) of S_{23}. (d) Magnitude (dB) of S_{31}.

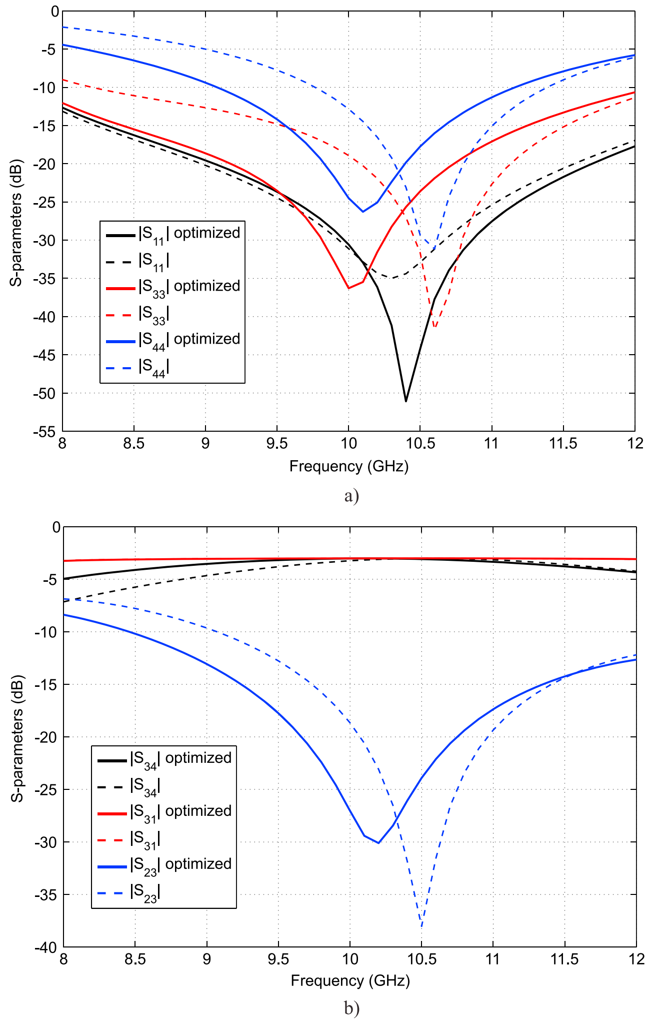

Figure 9. Magnitude of the S-parameters (dB) related to the redesigned magic-T junction considering $R = 4$ mm. (a) Magnitude of S_{11}, S_{33}, and S_{44}. (b) Magnitude of S_{34}, S_{31}, and S_{23}.

more evident in the present E-plane case (especially at low frequencies) for the cases $R = 4$ mm and $R = 4.5$ mm (note that, in such cases, the condition $R < b/4$ is not satisfied). As a consequence, a further optimization of the device is required in order to recover its wideband performance, and the main goal is to find a new electrical response as close as possible to the one obtained for the case $R = 0$.

The new obtained designs are shown in Figure 7, where the achieved electrical performance is, indeed, very close to the one we have derived for the case $R = 0$ (included in this case as a good reference curve). The new dimensions of the cylindrical post (located in a centered position) and the matching iris are shown in Table 2. The obtained results show that the developed CAD tool allows the microwave designer to accurately evaluate the final electrical response of the device prior to its manufacturing and compensate for the impact of the low-cost fabrication techniques by redesigning the dimensions of the matching elements (cylindrical post and iris). The CPU time required for the computation of a complete frequency response (150 points) was only 33.9 s (Ansys HFSS needed about 65 s per frequency point).

3.3. Design of Compensated Magic-T Junctions

In this section, the electrical performance of a compensated magic-T junction (see Figure 1) implemented in WR-90 rectangular waveguide is investigated. The component has been matched by means of a cylindrical metallic post ($r = 0.59$ mm, $h = 9.51$ mm, $x_0 = 11.43$ mm, $z_0 = 14.43$ mm) and an iris ($a_{iris} = 16.11$ mm, $t_{iris} = 1.36$ mm, $h_{iris} = 4.0$ mm). The S parameters of the device, taking into account the introduction of rounded corners of radius R in the rectangular waveguides of the component, are represented in Figure 8. The simulated

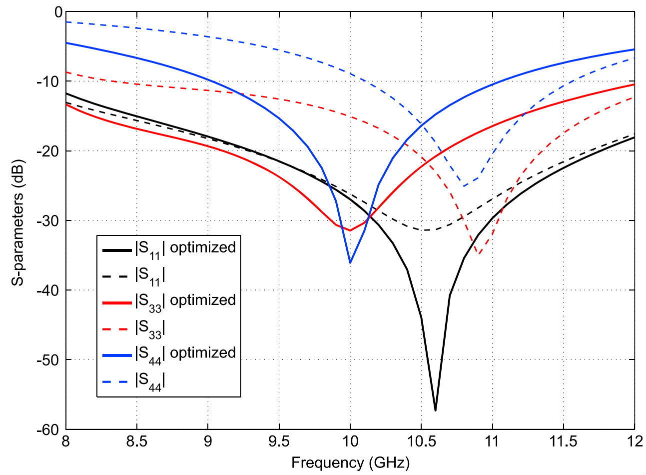

a)

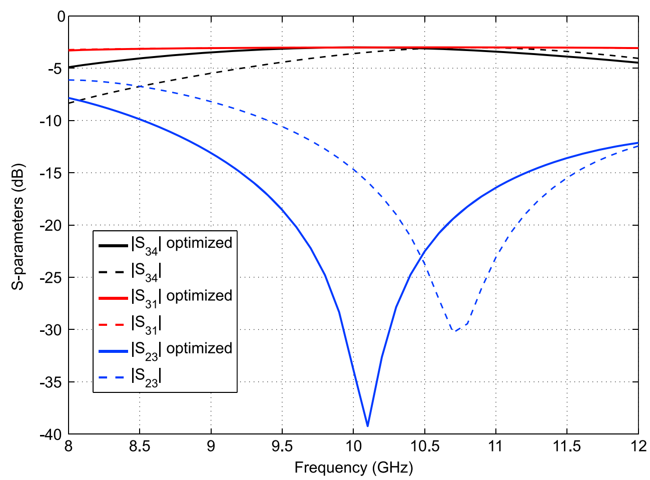

b)

Figure 10. Magnitude of the S-parameters (dB) related to the redesigned magic-T junction considering $R=5$ mm. (a) Magnitude of S_{11}, S_{33}, and S_{44}. (b) Magnitude of S_{34}, S_{31}, and S_{23}.

results have been successfully compared to the data provided by the commercial software Ansys HFSS, thus validating the implemented CAD tool. The negative impact on the electrical performance of the junction (frequency shift and deterioration of the S parameters), as the radius R of the rounded corners increases, is evident.

In order to minimize such degradation, a further optimization is carried out on the component for the cases $R = 4$ mm and $R = 5$ mm (where $R > b/4$), by redesigning the cylindrical post (its radius and height) and the matching iris. The S parameters related to the new designs have been represented in Figures 9 and 10. It is worth mentioning that the electrical performance of the magic-T junction has been improved in spite of employing high values for the radius of the rounded corners. The dimensions related to these new designs are displayed in Table 3 (note that, in this case, the relative position of the post has not been changed). Finally, the CPU time needed to compute a complete frequency response (150 points) was only 38.5 s (Ansys HFSS needed about 76 s per frequency point).

Table 3. New Dimensions of the Matching Elements (Post and Iris) Used in the Redesign of the Magic-T Junction

Radius R	r (mm)	h (mm)	a_{iris} (mm)	t_{iris} (mm)	h_{iris} (mm)
$R = 4$ mm	0.70	9.49	17.06	1.09	3.98
$R = 5$ mm	0.68	9.31	17.45	1.09	4.58

4. Conclusion

A rigorous and very efficient CAD tool for the analysis and design of compensated E-plane multiport junctions, which takes into account the presence of rounded corners in the rectangular waveguides of the device, has been proposed. The developed tool is based on well-known full-wave methods which assure the accuracy of the provided results. Several new designs concerning different E-plane components, such as right-angled bends, T-junctions, and magic-Ts, have been presented and discussed. The obtained results show that the implemented tool allows the designer to precisely predict the electrical performance of the device prior to its fabrication and compensate for the impact of the low-cost manufacturing techniques by redesigning the matching elements (i.e., cylindrical post and iris) considered in the device. Therefore, the wideband performance of the analyzed component can be almost restored even though stringent mechanical effects are imposed. The obtained numerical results have been successfully validated by comparison with simulated data provided by a commercial software tool based on the finite element method.

Acknowledgments
All the data necessary to understand, evaluate, replicate, and generate the figures and results presented in this paper have been included in the present manuscript. A full-wave custom code and the commercial software Ansys HFSS have been used to generate the simulated results provided by the authors. This work was supported by the Ministerio de Economía y Competitividad, Spanish Government, under the Research Projects TEC2013-47037-C5-1-R and TEC2013-47037-C5-4-R.

References

Arcioni, P. (1996), Fast evaluation of modal coupling coefficients of waveguide step discontinuities, *IEEE Microwave Guided Wave Lett.*, *6*(6), 232–234.

Arcioni, P., M. Bozzi, M. Bressan, G. Conciauro, and L. Perregrini (2002), Frequency/time-domain modeling of 3D waveguide structures by a BI-RME approach, *Int. J. Numer. Modell. Electron. Networks Devices Fields*, *15*(1), 3–21.

Berdnik, S. L., V. A. Katrich, M. V. Nesterenko, and Y. M. Penkin (2015), Waveguide E-plane T-junction with resonance coupling between shoulders, paper presented at 10th International Conference on Antenna Theory and Techniques, pp. 1–3, Kharkiv, Ukraine, 21–24 Apr.

Boria, V. E., and B. Gimeno (2007), Waveguide filters for satellites, *IEEE Microwave Mag.*, *8*(5), 60–70.

Cano, J. L., A. Mediavilla, S. Dragas, and A. Tazón (2016), Novel broadband circular waveguide four-way power divider for dual polarization applications, *IEEE Microwave Wireless Compon. Lett.*, *26*(2), 98–100.

Chen, C., L. Chen, and P. Zhao (2014), A waveguide diplexer based on E-plane T-junction, paper presented at 15th International Conference on Electronic Packaging Technology, pp. 1390–1391, Chengdu, China, 12–15 Aug.

Chu, Q. X., Q. S. Wu, and D. Y. Mo (2014), A Ka-band E-plane waveguide magic-T with coplanar arms, *IEEE Trans. Microwave Theory Tech.*, *62*(11), 2673–2679.

Cogollos, S., V. E. Boria, P. Soto, A. A. San-Blas, B. Gimeno, and M. Guglielmi (2003a), Direct computation of the admittance parameters of a cubic junction with arbitrarily shaped access ports using the BI-RME method, *IEE Proc. Microwaves Antennas Propag.*, *150*(2), 111–119.

Cogollos, S., S. Marini, V. E. Boria, P. Soto, A. Vidal, H. Esteban, J. V. Morro, and B. Gimeno (2003b), Efficient modal analysis of arbitrarily shaped waveguides composed of linear, circular, and elliptical arcs using the BI-RME method, *IEEE Trans. Microwave Theory Tech.*, *51*(12), 2378–2390.

Conciauro, G., M. Bressan, and C. Zuffada (1984), Waveguide modes via an integral equation leading to a linear matrix eigenvalue problem, *IEEE Trans. Microwave Theory Tech.*, *32*(11), 1495–1504.

Gerini, G., M. Guglielmi, and G. Lastoria (1998), Efficient integral equation formulations for the computation of the multimode admittance or impedance matrix of planar waveguide junctions, paper presented at IEEE MTT-S International Microwave Symposium, pp. 1747–1750, Baltimore, United States.

Helszajn, J. (2016), The electrically symmetrical E-plane waveguide tee junction at the Dicke and Altman planes, *IEEE Trans. Microwave Theory Tech.*, *64*(3), 715–723.

Hirokawa, J., K. Sakurai, M. Ando, and N. Goto (1991), An analysis of a waveguide T junction with an inductive post, *IEEE Trans. Microwave Theory Tech.*, *39*(3), 563–566.

Kamandi, M., S. Emadi, and R. Faraji-Dana (2015), Integral equation analysis of multilayered waveguide bends using complex images Green's function technique, *J. Lightwave Technol.*, *33*(9), 1774–1779.

Leal-Sevillano, C. A., J. A. Ruiz-Cruz, J. R. Montejo-Garai, and J. M. Rebollar (2013), Compact broadband couplers based on the waveguide magic-T junction, paper presented at 43rd European Microwave Conference, pp. 151–154, Nuremberg, Germany, 6–10 Oct.

Mira, F., M. Bressan, G. Conciauro, B. Gimeno, and V. E. Boria (2005), Fast S-domain method of rectangular waveguides with radially-symmetric metal insets, *IEEE Trans. Microwave Theory Tech.*, *53*(4), 1294–1303.

Park, S. G., H. Lee, and Y. H. Kim (2009), A turnstile junction waveguide orthomode transducer for the simultaneous dual polarization radar, paper presented at 2009 Asia Pacific Microwave Conference, pp. 135–138, Singapore, 7–10 Dec.

Ruiz, J., P. Soto, V. E. Boria, and A. A. San-Blas (2015), Compensated double-ridge waveguide E-plane and H-plane T-junctions, paper presented at 2015 IEEE 15th Mediterranean Microwave Symposium (MMS), pp. 175–178, Lecce, Italy, 30 Nov.–2 Dec.

San-Blas, A. A., F. Mira, V. E. Boria, B. Gimeno, M. Bressan, and P. Arcioni (2007), On the fast and rigorous analysis of compensated waveguide junctions using off-centered partial-height metallic posts, *IEEE Trans. Microwave Theory Tech.*, *55*(1), 168–175.

San-Blas, A. A., V. E. Boria, B. Gimeno, and S. Cogollos (2015), Design of compensated multiport waveguide junctions considering mechanization effects, *AEU Int. J. Electron. Commun.*, *69*(1), 328–331.

Uher, J., J. Bornemann, and U. Rosenberg (1993), *Waveguide Components for Antenna Feed Systems: Theory and CAD*, Norwood, Mass., Artech House.

Xu, Z., J. Xu, Y. Cui, and C. Qian (2015), A novel rectangular waveguide T-junction for power combining application, *IEEE Microwave Wireless Compon. Lett.*, *25*(8), 529–531.

Zhang, D., Y. Zhao, W. Liu, W. Zhao, and Q. Sun (2010), A fast synthesis approach for diplexer with E-plane T-junction design, paper presented at 3rd International Symposium on Information Science and Engineering, pp. 133–136, Shangai, China, 24–26 Dec.